Epidermal Growth Factor Receptor–Targeted Immunoliposomes Significantly Enhance the Efficacy of Multiple Anticancer Drugs *In vivo*

Christoph Mamot,[1,2] Daryl C. Drummond,[3,4] Charles O. Noble,[1,3] Verena Kallab,[1] Zexiong Guo,[3] Keelung Hong,[3,4] Dmitri B. Kirpotin,[3,4] and John W. Park[1]

[1]Division of Hematology-Oncology, University of California at San Francisco, San Francisco, California; [2]Department of Research and Division of Oncology, University Hospital of Basel, Basel, Switzerland; [3]California Pacific Medical Center Research Institute, Liposome Research Laboratory; and [4]Hermes Biosciences, Inc., South San Francisco, California

Abstract

We previously reported the development of epidermal growth factor receptor (EGFR)–targeted immunoliposomes that bind and internalize in tumor cells which overexpress EGFR and/or mutant EGFR variant III (EGFRvIII), enabling intracellular delivery of potent anticancer agents *in vitro*. We now describe *in vivo* proof-of-concept for this approach for the delivery of multiple anticancer drugs in EGFR-overexpressing tumor models. Anti-EGFR immunoliposomes were constructed modularly with Fab′ fragments of cetuximab (IMC-C225), covalently linked to liposomes containing probes and/or anticancer drugs. Pharmacokinetic and biodistribution studies confirmed long circulation times ($t_{1/2}$ = 21 hours) and efficient accumulation in tumors (up to 15% ID/g) irrespective of the presence of the targeting ligand. Although total accumulations of anti-EGFR immunoliposomes and nontargeted liposomes in EGFR-overexpressing tumors were comparable, only immunoliposomes internalized extensively within tumor cells (92% of analyzed cells versus <5% for nontargeted liposomes), indicating different mechanisms of delivery at the cellular level. *In vivo* therapy studies in a series of xenograft models featuring overexpression of EGFR and/or EGFRvIII showed the superiority of immunoliposomal delivery of encapsulated drugs, which included doxorubicin, epirubicin, and vinorelbine. For each of these drugs, anti-EGFR immunoliposome delivery showed significant antitumor effects and was significantly superior to all other treatments, including the corresponding free or liposomal drug (P < 0.001-0.003). We conclude that anti-EGFR immunoliposomes provide efficient and targeted drug delivery of anticancer compounds and may represent a useful new treatment approach for tumors that overexpress the EGFR. (Cancer Res 2005; 65(24): 11631-8)

Introduction

Nanoparticles, including liposomes and other nanoscale constructs, can be used to deliver drugs to tumors. Certain nanoparticles, such as sterically stabilized liposomes, have already been optimized for prolonged circulation and redirection of drug, which can yield superior accumulation in tumors via a process often referred to as the "enhanced permeability and retention" effect (for review, see refs. 1, 2). Notable examples are the liposomal anthracyclines pegylated liposomal doxorubicin (PLD; Doxil/Caelyx) and liposomal daunorubicin (DaunoXome), both of which are currently approved for cancer treatment.

Immunoliposomes, in which monoclonal antibody (mAb) fragments are conjugated to liposomes, represent the next generation of molecularly targeted drug delivery systems. By combining the tumor targeting properties of mAbs with the pharmacokinetics and drug delivery advantages of liposomes, immunoliposomes offer the promise of selective drug delivery to tumor cells, including internalization and intracellular drug release within targeted cells (3). For example, we previously reported that immunoliposomes that bind to and internalize in HER2-overexpressing tumor cells (4, 5) show significantly increased therapeutic efficacy in delivering doxorubicin in preclinical tumor models (6) and can be manufactured from existing liposomal doxorubicin (7, 8).

We have also developed immunoliposomes that target epidermal growth factor receptor (EGFR; ErbB), which is involved in the pathogenesis of many tumors and is a proven target for cancer therapy (for review, see ref. 9). Anti-EGFR immunoliposomes were constructed using Fab′ fragments of mAb C225 (cetuximab, Erbitux), a chimeric anti-EGFR mAb that is in clinical use for colorectal cancer treatment, as well as scFv C10, an independently derived phage antibody; these immunoliposomes mediated specific and efficient intracellular drug delivery to a variety of target cells *in vitro* (10). Here we describe *in vivo* properties of anti-EGFR immunoliposomes, including the therapeutic potential of this receptor-targeted vehicle for the delivery of various cytotoxic drugs in a series of EGFR-overexpressing tumor models.

Materials and Methods

Liposome preparation. Liposomes were prepared by a lipid film hydration-extrusion method using repeated freeze-thawing to hydrate the lipid films (11). Liposomes were composed of 1,2-distearoyl-*sn*-glycero-3-phosphocholine (DSPC) and cholesterol (molar ratio 3:2) with methoxy polyethylene glycol (mPEG)-1,2-distearoyl-3-*sn*-glycerophosphoethanolamine (DSPE; 0.5-5 mol% of phospholipid; Avanti Polar Lipids; Alabaster, AL). Following hydration, liposomes were extruded 10 times through polycarbonate filters (0.1 μm pore size), followed by extrusion seven times through additional filters (0.08 μm pore size). Liposome size was determined by dynamic light scattering (typically 80-100 nm). Phospholipid concentration was measured by phosphate assay (12).

For liposomes loaded with ADS645WS (American Dye Source, Quebec, Canada), the fluorescent dye (5 mmol/L) was dissolved in buffer for rehydration of the dried lipids. After passive loading, unencapsulated dye was removed using Sephadex G-75 chromatography.

For encapsulation of chemotherapeutic drugs doxorubicin (Bedford Laboratories, Bedford, OH) and epirubicin (Pharmacia, Kalamazoo, MI), a standard remote-loading method using ammonium sulfate was done

Requests for reprints: John W. Park, Division of Hematology-Oncology, University of California at San Francisco, 2nd Floor, 1600 Divisadero Street, San Francisco, CA 94115. Phone: 415-502-3844; Fax: 415-353-9571; E-mail: jpark@cc.ucsf.edu.

doi:10.1158/0008-5472.CAN-05-1093

(13, 14). For encapsulation of vinorelbine, liposomes were prepared as described following hydration in a solution of triethylammonium sucrose octasulfate (TEA_8SOS; 0.65 mol/L TEA, pH 5.2-5.5). Unentrapped TEA_8SOS was removed on a Sepharose CL-4B size exclusion column. Vinorelbine was added at a drug-to-phospholipid ratio of 350 g drug/mol phospholipid and the pH adjusted to 6.5 with 1 N HCl before initiation of loading at 60°C for 30 minutes. The resulting liposomal vinorelbine was purified on a Sephadex G-75 column to remove unencapsulated drug.

Preparation of monoclonal antibody fragments and immunoliposomes. Intact C225 mAb (cetuximab, Erbitux; ImClone Systems, Inc., New York, NY) was cleaved and reduced as previously described (10). Fab′ fragments were covalently conjugated to maleimide groups at the termini of PEG-DSPE chains (Mal-PEG-DSPE; Nektar, Huntsville, AL; ref. 8). Conjugation efficiencies were typically 30% to 50% for C225-Fab′. For incorporation into preformed liposomes or commercial PLD (Doxil; Alza Pharmaceuticals, Palo Alto, CA), mAb conjugates were incorporated into liposomes by coincubation at 55°C for 30 minutes at protein/liposome ratio of 30 μg Fab′/μmol phospholipid, resulting in incorporation efficiencies of 70% to 80% (10).

Pharmakokinetic studies. Healthy adult Sprague-Dawley rats (CD IGS rats, Charles River Laboratories, Wilmington, MA) received single i.v. injections of liposomes or immunoliposomes loaded with doxorubicin (5 mg doxorubicin/kg). For two-component pharmacokinetic studies, serial blood samples were divided and analyzed for both doxorubicin and [^{3}H]-cholesteryl hexadecyl ether [cholesteryl-1,2-^{3}H(N); Perkin-Elmer, Boston, MA] as a liposome marker. Plasma concentrations of doxorubicin were determined by fluorescence and those of liposomes by radioactivity counting. Construct stability in circulation was evaluated by serial determinations of the doxorubicin-to-lipid ratio. Noncompartmental pharmacokinetic data analysis was done using PK Solutions 2.0 software (Summit Research Services, Montrose, CO).

Biodistribution studies. NCR *nu/nu* mice (5-6 weeks; Taconic, Germantown, NY) were injected s.c. with EGFR-overexpressing MDA-MB-468 tumor cells (2×10^7 cells) in the dorsum of the animal. When tumor xenografts were fully established and had reached volumes of 400 to 800 mm^3, animals were randomly assigned to different treatment groups: 3 mice per group × 2 groups (EGFR-targeted and nontargeted) × 2 time points (24 and 72 hours). Liposomes or anti-EGFR immunoliposomes, both loaded with doxorubicin and labeled with [^{3}H]-cholesteryl hexadecyl ether, were injected i.v. via tail vein at a dose of 5 mg doxorubicin/kg. At 24 or 72 hours, animals were euthanized and tissues were collected following perfusion with PBS and analyzed for doxorubicin and lipid. Tissue samples were homogenized and drug (doxorubicin) and lipid (liposomes) concentrations were determined as described. The final distribution was expressed as percentage of injected dose for the concentration in circulation (blood) and as % of injected dose/g of tissue for all other samples. Analyses were done in triplicate; data indicate mean ± SD.

***In vivo* uptake studies.** Nude mice (NCR *nu/nu*) were injected s.c. with U87 glioblastoma cells (1×10^7) additionally transfected with EGFR variant III (EGFRvIII; ref. 15). Once tumors size reached 400 to 800 mm^3, animals were randomly assigned to treatment group: 3 mice per group × 3 groups (saline, nontargeted, and EGFR-targeted liposomes). Liposomes and immunoliposomes loaded with the fluorophore ADS645WS were injected i.v. as a single dose via tail vein (total 10 μmol phospholipid/animal in 200 μL volume). After 24 hours, animals were euthanized and tumors were excised and disaggregated [1 hour at 37°C in 0.1% (w/v) collagenase IV (Sigma, St. Louis, MO) and 0.003% DNase I (Calbiochem, San Diego, CA)]. Cell suspensions were carefully washed, fixed [formaldehyde, 1% (v/v)], and analyzed by flow cytometry (FACSCalibur2, BD Biosciences, Inc., San Jose, CA) or confocal microscopy (LSM 510 meta, Carl Zeiss, Inc., Thornwood, NY).

Tumor xenograft models. Tumor cells (MDA-MB-468, U87, or U87vIII) were injected in the dorsum of nude mice as described. Once tumor xenografts had become established and 150 to 400 mm^3 in volume, mice were randomly assigned to treatment groups (10-15 animals per group). Liposomes and immunoliposomes were administered via tail vein at approximate maximum tolerated dose (MTD) once weekly for 3 weeks. Based on typical drug/lipid ratios of 150 μg drug/μmol phospholipid, the corresponding lipid dose was typically 0.8 to 1.3 μmol of phospholipid per injected dose and 2.4 to 3.9 μmol total. "Empty" anti-EGFR immunoliposomes were prepared identically, except for omission of cytotoxic drug, and were administered i.v. at the same lipid dose as anti-EGFR immunoliposomal drugs. Free drug and saline were injected on the same schedule as liposomes/immunoliposomes. Free mAb C225 was injected i.p. at 1 mg/dose twice a week for 3 weeks according to optimized regimens (16).

Tumor measurements were done [(length × width^2) / 2] and mice were weighed and examined for toxicity thrice a week for 60 to 90 days post tumor implantation. Mice with complete clinical regressions were examined histopathologically and were classified as "cured" if no residual tumor was detected after histopathologic analysis.

Statistical analysis. Treatment effects were compared using Student's t test (two-sample individual t test) for tumor size at each time point. In addition, a multivariate (rank) test was done based on the sums of ranks for each mouse. Tumor sizes at each time point following final injection were ranked across all mice and the ranks were summed. The sum of the ranks was compared in each case for two treatments by a two-sample t test (17).

Results

Construction of immunoliposomal drugs targeted to EGFR. Immunoliposomes were constructed using a modular design that builds on sterically stabilized liposomes optimized for long circulation as drug-containing nanoparticles as previously described (3, 4, 10). Briefly, conjugation was done by covalent linkage of Fab′ fragments derived from mAb C225 to modified termini of PEG chains on liposomes (5) or by covalent linkage to Mal-PEG-DSPE linker in solution, followed by incorporation of the resulting micellar conjugates into liposomes (18). The "micellar incorporation" method allowed stable addition of numerous mAb fragments to an existing drug-loaded liposome such as PLD (Doxil/Caelyx).

For delivery of other drugs, novel nanoparticle/liposome-based constructs were prepared using a new process for active drug loading and retention. Previous methods for liposome drug loading have been extremely variable, with excellent results with liposomal anthracyclines (14) but more problematic efficiency and/or stability with other drugs (19). In this new technique, liposomes were formed with an entrapped solution containing poorly permeable ionic species such as substituted ammonium salts of poly(phosphate) or sucrose octasulfate, and then transferred to a buffer solution containing the drug. The resulting transmembrane potential induced spontaneous accumulation of weakly basic drugs into the liposome interior, producing packing, gelation, or crystallization of drug within the liposome. This technique enabled highly robust encapsulation of a number of chemical classes into stabilized liposomes, including epirubicin, *Vinca* alkaloids, ellipticines, and camptothecins; the resulting constructs were notable for extremely efficient loading (~100% of added drug was encapsulated), unsurpassed drug yields (10^4-10^5 drugs per particle), and marked *in vivo* stability (20, 21). In this report, we converted new liposomal constructs of epirubicin and vinorelbine into immunoliposome versions targeted to EGFR.

Pharmacokinetics of anti–EGFR immunoliposome-doxorubicin. Pharmacokinetic studies of anti-EGFR immunoliposome-doxorubicin were done in healthy adult rats. Immunoliposomes or matched liposomes lacking mAb fragments were labeled with [^{3}H]-cholesteryl hexadecyl ether and loaded with doxorubicin. After a single i.v. dose, anti-EGFR immunoliposome-doxorubicin showed prolonged circulation of both lipid and drug components, both of

which were still present at ~20% of 5-minute levels at 48 hours postinjection (Fig. 1*A*). In contrast, free doxorubicin at the same dose was already undetectable at 4 hours postinjection. These data confirmed that immunoliposome delivery greatly extended the circulation time of encapsulated doxorubicin and that carrier and drug circulated together without appreciable drug release. Furthermore, the pharmacokinetics of immunoliposome components were indistinguishable from those of sterically stabilized liposomal doxorubicin, indicating that mAb fragment conjugation did not compromise circulation time or stability. Plasma clearances for liposomal and immunoliposomal doxorubicin were equivalent at 2.48 ± 0.21 and 2.74 ± 0.25 mL/h, as were the areas under the plasma concentration versus time curve at 2,025 ± 170 and 1,836 ± 165 μg h/mL, respectively (Table 1). Similarly, serial measurements of the doxorubicin-to-phospholipid ratio, indicative of drug retention, were equivalent at all time points. For example, the doxorubicin-to-phospholipid ratio at 48 hours was 89.14 ± 0.39 for nontargeted liposomal doxorubicin and 84.67 ± 1.92 for anti-EGFR immunoliposome-doxorubicin.

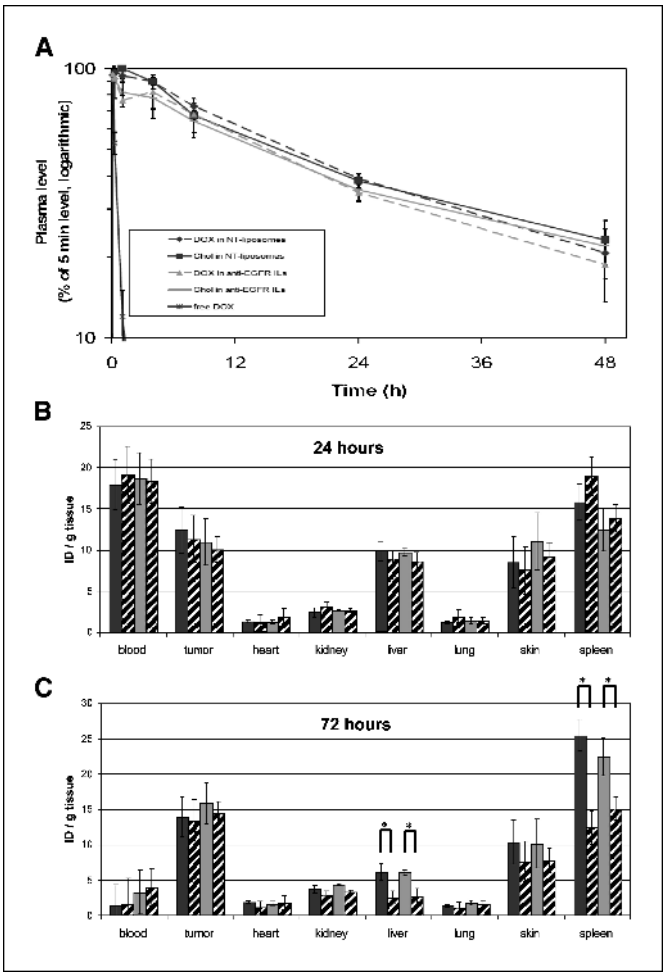

Figure 1. Pharmacokinetics and biodistribution of anti-EGFR immunoliposomes. Sterically stabilized liposomes were prepared with 10% PEG-DSPE and ^{3}H-Chol [cholesteryl-1,2-^{3}H(N)], then loaded with doxorubicin and conjugated or not to C225-Fab′. *A,* pharmacokinets in adult rats. Free doxorubicin (*DOX*), nontargeted liposomal doxorubicin, or anti-EGFR immunoliposomal doxorubicin was injected i.v. into normal healthy adult rats (three rats per group) at a dose of 5 mg doxorubicin/kg. Lipid [cholesteryl-1,2-^{3}H(N); *solid lines*] and doxorubicin (*dotted lines*) were separately assayed at the indicated times. Injection of free doxorubicin resulted in no detectable drug after 4 hours (<2.5% ID). *Points,* mean; *bars,* SD. *B* and *C,* MDA-MB-468 xenograft model. EGFR-overexpressing MDA-MB-468 cells were implanted s.c. in nude mice. Either nontargeted liposomal doxorubicin (*black columns*) or anti-EGFR immunoliposomal doxorubicin (*gray columns*) was injected i.v. at a dose of 5 mg doxorubicin/kg. Lipid [cholesteryl-1,2-^{3}H(N); *solid columns*] and doxorubicin (*hatched columns*) were separately assayed in the indicated tissues at 24 hours (*B*) or 72 hours (*C*) posttreatment (n = 3). Data for blood samples are expressed as % ID; for all other tissues, data are expressed as % ID/g tissue. *, $P < 0.05$; comparison of lipid versus doxorubicin levels showed significant differences in liver and spleen at 72 hours (two-sample individual t test), reflecting drug metabolism. *Columns,* mean; *bars,* SD.

Biodistribution of anti–EGFR immunoliposomes versus nontargeted liposomes. Biodistribution and tumor tissue localization of liposomal and immunoliposomal doxorubicin were evaluated in nude mice bearing EGFR-overexpressing MDA-MB-468 breast tumor xenografts. Following a single i.v. injection of either liposomes or immunoliposomes, deliveries of liposomal lipid ([^{3}H]-cholesteryl hexadecyl ether) and encapsulated drug (doxorubicin) were separately assayed in various tissues at 24 or 72 hours (Fig. 1*B* and *C*).

At 24 hours, tissue levels for both anti-EGFR immunoliposomes and nontargeted liposomes were highest in blood, consistent with the long circulation times observed in rats. Blood levels were slightly lower in tumor-bearing nude mice than in normal rats: 18% ID to 20% ID for tumor-bearing mice versus >40% ID for rats at 24 hours postinjection. This differential may reflect species-specific differences in pharmacokinetics as well as an increase in clearance in tumor-bearing animals. These results again showed equivalent circulation times for immunoliposomes and liposomes, with no compromise in pharmacokinetics due to the presence of mAb fragments.

In addition to high blood levels, at 24 hours, both nanoparticles reached high levels in tumor, liver, spleen and skin. Accumulation in other organs, including heart, lung and kidney, was substantially lower. This biodistribution pattern is fully consistent with the well-established preclinical and clinical profile of sterically stabilized liposomes, such as PLD, which feature reduced but eventual clearance in reticuloendothelial system (RES) sites in liver and spleen (22).

At 72 hours, blood levels of both nanoparticles showed a decline whereas tumor levels increased and RES sites showed a more complex pattern. In liver and spleen, levels of cholesterol and doxorubicin, which were equivalent at 24, showed a relative decrease in doxorubicin as compared with cholesterol at 72 hours ($P < 0.05$). This result likely reflected metabolism and clearance of doxorubicin within the RES between 24 and 72 hours.

Importantly, tumor accumulation in EGFR-overexpressing MDA-MB-468 tumor cells was extremely high for nontargeted liposomes and was not further increased in the case of anti-EGFR immunoliposomes. At 24 hours, tumor levels for both nanoparticles reached 10% to 12% ID/g tissue, and continued to accumulate at 72 hours to 13% to 15% ID/g tissue. The observation that mAb-mediated targeting did not further increase accumulation of long circulating liposomes in tumors is consistent with previous results using anti-HER2 immunoliposomes in HER2-overexpressing tumor models (4, 23).

Internalization of anti–EGFR immunoliposomes in xenografted tumor cells *in vivo*. Although anti-EGFR immunotargeting did not confer additional tumor tissue localization, we evaluated whether the mAb component was capable of mediating binding and internalization of immunoliposomes in tumor cells *in vivo* as we reported previously in *in vitro* studies. Confocal microscopy was used to compare binding and uptake of EGFR-targeted immunoliposomes and nontargeted liposomes in the U87/EGFRvIII tumor model, which overexpresses both EGFR and

Table 1. Plasma pharmacokinetics of free, liposomal, and anti-EGFR immunoliposomal doxorubicin in adult rats

Treatment*	$t_{1/2}$ (h)	AUC_∞ (μg h/mL)	CL (mL/h)	V_d (mL)	MRT (h)	DOX-to-PL† (%ID/%ID)
Ls-DOX	21.5 ± 2.0	2,025 ± 170	2.48 ± 0.21	76.5 ± 0.7	31.0 ± 2.8	89.14 ± 0.39
Anti-EGFR ILs-DOX	20.7 ± 3.3	1,836 ± 165	2.74 ± 0.25	81.1 ± 5.9	29.9 ± 4.9	84.67 ± 1.92

Abbreviations: AUC_∞, area under the plasma concentration versus time curve based on the sum of exponential terms; MRT, mean residence time calculated from exponential terms; CL, clearance calculated from exponential terms; V_d, volume of distribution.
*Liposomal doxorubicin (Ls-DOX) and anti-EGFR immunoliposome-doxorubicin (Anti-EGFR ILs-DOX) were prepared using DSPC/Chol/PEG-DSPE (3:2:0.3, mol/mol/mol) and loaded with doxorubicin at a ratio of 150 g doxorubicin/mol phospholipid using the ammonium sulfate gradient-loading method as described in Materials and Methods. Anti-EGFR immunoliposome-doxorubicin or nontargeted liposomes were administered i.v. at a single dose of 5 mg doxorubicin/kg; two animals per group.
†Ratio of doxorubicin-to-phospholipid at the 48-hour time point.

EGFRvIII. For these studies, liposomes were loaded with the water-soluble fluorescent dye ADS645WS, with or without mAb fragments, and administered in tumor-bearing mice as a single-dose i.v. injection. At 24 hours postinjection, tumors were removed, disaggregated, and extensively washed for analysis. Confocal microscopy of the treated and harvested tumor cells showed that anti-EGFR immunoliposomes had accumulated profusely throughout the cytoplasm in a pattern consistent with receptor-mediated endocytosis (Fig. 2*A*). In contrast, control liposomes lacking the mAb fragment showed only minimal binding or uptake (Fig. 2*B*), which did not seem to be significantly different than the background (Fig. 2*C*).

Quantitative analysis of cellular accumulation of immunoliposomes following i.v. administration was done using a flow cytometry assay. Twenty-four hours following i.v. injection of ADS645WS-loaded immunoliposomes or liposomes, disaggregated cells from U87 xenografts were gated for positive nuclear staining and evaluated for fluorescence uptake. Overall, anti-EGFR immunoliposomes achieved cellular uptake that was 6-fold greater than that of nontargeted liposomes (Fig. 2*D*). Tumors were also characterized in separate experiments by *ex vivo* analysis of the cell population. Tumors were excised from mice that did not receive i.v. treatment and processed as described; the resulting cell suspension was then incubated for 2 hours at 37°C with ADS645WS-loaded anti-EGFR immunoliposomes or nontargeted liposomes *ex vivo*. Immunoliposome uptake was observed in 92% of the population (Fig. 2*E*) whereas nontargeted liposomes showed minimal uptake in <5% of the population (Fig. 2*F*). These results confirmed that the preponderance of the analyzed cells in harvested tumor tissues consisted of tumor cells capable of taking up anti-EGFR immunoliposomes.

Taken together, these studies indicated that immunoliposomes and nontargeted liposomes were comparable in overall tumor tissue localization but, at the cellular level, displayed distinctly different mechanisms of delivery. Consistent with *in vitro* results, anti-EGFR immunoliposomes, but not liposomes, were capable of extensive cellular uptake and internalization in EGFR-overexpressing tumor cells *in vivo*.

Efficacy of anti–EGFR immunoliposomal doxorubicin in EGFR–overexpressing tumor xenograft models. The therapeutic efficacy of EGFR-targeted immunoliposomes containing doxorubicin (anti-EGFR immunoliposome-doxorubicin) was evaluated in two different EGFR-overexpressing tumor xenograft models: MDA-MB-468 human breast tumors ($\sim 5 \times 10^5$ receptors per cell) and U87 human glioblastoma tumors ($\sim 1 \times 10^5$-2×10^5 receptors per cell). In both models, 1×10^7 to 2×10^7 tumor cells were implanted s.c. without matrigel in the flank of nude mice and allowed to grow until fully established and substantial in volume. To rigorously evaluate anticancer efficacy against advanced tumors, treatments were initiated when tumors were moderately large (mean volume, >150 mm^3) or extremely large (mean volume, >400 mm^3). We then evaluated the therapeutic effects of anti-EGFR immunoliposomal doxorubicin alongside various comparators.

In the MDA-MB-468 xenograft model with moderate-sized tumors (>150 mm^3), anti-EGFR immunoliposome-doxorubicin was administered i.v. at a total dose of 15 mg doxorubicin/kg divided over three weekly doses of 5 mg/kg/wk (Fig. 3*A*). Other treatments included saline, free doxorubicin at its MTD of 7.5 mg/kg, nontargeted liposomal doxorubicin (commercial PLD) at the same dose and schedule as immunoliposomes, and irrelevant immunoliposomes containing a different mAb fragment not specific for EGFR, also at the same dose and schedule as anti-EGFR immunoliposomes.

As expected, free doxorubicin produced some tumor growth inhibition as compared with saline treatment. Both nontargeted liposome delivery via PLD and irrelevantly targeted immunoliposome-doxorubicin showed increased efficacy over free drug [$P < 0.0001$, multivariate (rank) test]; this is consistent with the established advantages of liposome delivery of anthracyclines in preclinical models (19). Treatment with anti-EGFR immunoliposome-doxorubicin produced substantial tumor regressions and was the most efficacious treatment. Because immunoliposomes were prepared by conjugation of Fab′ to PLD itself, the superiority of anti-EGFR immunoliposome-doxorubicin ($P < 0.001$ versus PLD) was clearly due to targeting by the anti-EGFR mAb fragments. In addition, cured tumors, defined as complete eradication of tumor during treatment and confirmed by histopathology at sacrifice, occurred in 27% (3 of 11) of immunoliposome-treated mice versus 0% for all other treatments, including free doxorubicin (0 of 10), nontargeted PLD (0 of 11), and irrelevantly targeted PLD (0 of 10). This represented a statistically significant advantage for anti-EGFR immunoliposome-doxorubicin versus either nontargeted or irrelevantly targeted PLD ($P = 0.011$, individual two-sample t tests).

Anti-EGFR immunoliposome-doxorubicin was further evaluated in a different EGFR-overexpressing tumor model featuring U87 human glioblastoma xenografts (Fig. 3*B*). In this highly tumorigenic and rapidly growing model, treatment was initiated against very large U87 tumors (~ 450 mm^3). Despite this, anti-EGFR

immunoliposome-doxorubicin produced substantial tumor growth inhibition and was clearly superior to all other treatments, including nontargeted PLD (P = 0.002), free doxorubicin (P < 0.001), and saline.

As an additional control, one group of mice received treatment with empty anti-EGFR immunoliposomes lacking encapsulated drug. Empty anti-EGFR immunoliposomes, administered i.v. at the same lipid dose and schedule as anti-EGFR immunoliposome-doxorubicin, produced no measurable effect on tumor growth. This result indicated that the potent activity of anti-EGFR immunoliposome-doxorubicin was due to targeted delivery of doxorubicin and not to the antiproliferative activity of C225-Fab′

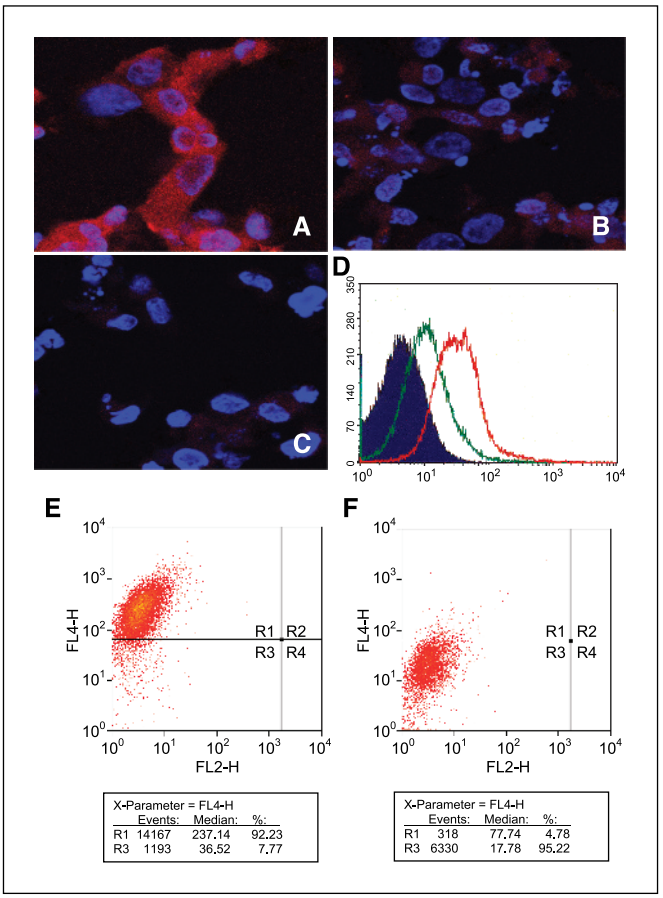

Figure 2. *In vivo* uptake of liposomes and immunoliposomes in the U87/EGFRvIII tumor xenograft model. U87/EGFRIII tumor cells, overexpressing EGFR and EGFRvIII, were implanted s.c. in nude mice. After tumors had become fully established, mice received a single i.v. injection of saline, nontargeted liposomes, or anti-EGFR immunoliposomes. Liposomes and immunoliposomes were loaded with the fluorescent marker ADS645WS. At 24 hours, tumor cells were harvested by tissue disaggregation, extensive washing, and resuspension. Tumor cell uptake of liposomes or immunoliposomes was evaluated by confocal microscopy and flow cytometric analysis: *A,* tumor cells showing uptake of anti-EGFR immunoliposomes; *B,* tumor cells showing no apparent uptake of nontargeted liposomes; *C,* tumor cells treated with saline; *D,* flow cytometric analysis showing greater uptake of anti-EGFR immunoliposomes (*red*) as compared with nonspecific accumulation of nontargeted liposomes (*green*). Events were gated for positive nuclear staining. In separate control experiments, cell suspensions were derived from mice that did not receive i.v. treatment and processed as described, and then incubated *ex vivo* for 2 hours at 37°C with either ADS645WS-loaded anti-EGFR immunoliposomes (*E*) or nontargeted liposomes (*F*). Flow cytometry was done to evaluate immunoliposome/liposome uptake in the cell suspension and the proportion of cells positive or negative for uptake was calculated using the gates shown. Representative results from two therapy experiments (*A-D*; three animals per group) and four control experiments (*E-F*; one animal per study).

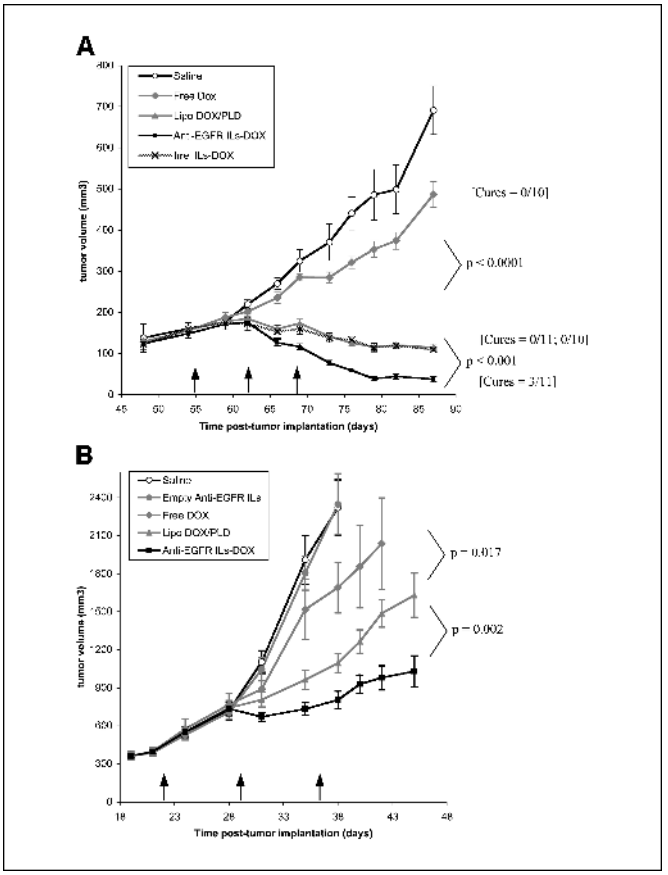

Figure 3. Therapeutic efficacy of anti-EGFR immunoliposome-doxorubicin in EGFR-overexpressing tumor models. *A,* MDA-MB-468 model. Anti-EGFR immunoliposomes containing doxorubicin (*Anti-EGFR ILs-DOX*; ■) were administered i.v. at a total dose of 15 mg doxorubicin/kg on the indicated days post tumor implantation (*arrows*). Other treatment groups included saline (○), free doxorubicin (◇) at its MTD of 7.5 mg/kg, PLD (*Lipo Dox/PLD*; ♦) at 15 mg/kg, and irrelevant immunoliposomes (*Irrel ILs-DOX*; ×) containing a mAb fragment not specific for EGFR. Ten to eleven mice in each group. Liposome delivery was significantly superior to free drug (P < 0.0001) whereas anti-EGFR immunoliposome-doxorubicin was in turn significantly superior to nontargeted liposomal doxorubicin (P < 0.001). *B,* U87 model. Anti-EGFR immunoliposome-doxorubicin (■) was administered i.v. at a total dose of 15 mg doxorubicin/kg over three weekly doses on the indicated days post tumor implantation (*arrows*). Other treatment groups included saline (○), free doxorubicin (◇) at its MTD of 7.5 mg/kg, PLD (*Lipo Dox/PLD*; ♦) at 15 mg/kg, and anti-EGFR immunoliposome-doxorubicin identically prepared but lacking doxorubicin (*Empty Anti-EGFR ILs*; ●). Ten to twelve mice in each group. Liposome delivery was significantly superior to free drug (P = 0.017) whereas anti-EGFR immunoliposome-doxorubicin was in turn significantly superior to nontargeted PLD (P = 0.002). *Points,* mean tumor volumes; *bars,* SE. P values were based on a multivariate (rank) test for the indicated treatment groups.

fragments present on the immunoliposomes. These results are also consistent with previous studies of anti-HER2 immunoliposomes containing trastuzumab-based Fab′, which showed no antitumor efficacy when empty unless administered at much more frequent intervals to achieve steady-state concentrations of the mAb component (6).

Anti-EGFR immunoliposome-doxorubicin was well tolerated by the mice. Maximum weight loss was 6.3 ± 3.5% for anti-EGFR immunoliposome-doxorubicin and 4.6 ± 3.9% for Food and Drug Administration–approved PLD, which were not statistically different (individual two-sample t tests).

Efficacy of anti–EGFR immunoliposome-epirubicin in an EGFR/EGFRvIII–overexpressing tumor xenograft model. EGFRvIII (ΔEGFR), an in-frame deletion of the extracellular domain

associated with constitutive signaling, has been detected in many gliomas and other tumors (24–30); it seems to play a role in glioma tumorigenesis although its role in other tumor types is less clear (31).

Anti-EGFR immunoliposomes constructed from either C225-Fab′ or scFv C10 can target EGFRvIII-expressing tumor cells as their epitopes are retained in the truncated receptor (10). Anti-EGFR immunoliposomes were evaluated in the U87/EGFRvIII tumor xenograft model in which U87 human glioma cells were stably transfected with mutant EGFRvIII (15). Coexpression at high levels of wild-type EGFR ($\sim 1 \times 10^5$-2×10^5 receptors per cell) and mutant EGFRvIII ($\sim 5 \times 10^5$ receptors per cell) in this model corresponds to a frequent phenotype in human gliomas and possibly other tumors (25).

For these studies, liposomes and anti-EGFR immunoliposomes were loaded with the anthracycline drug epirubicin. As a free drug, epirubicin has potential advantages over doxorubicin, including possibly reduced cardiotoxicity (32). Liposome delivery has also been shown to reduce this important limitation of doxorubicin (33, 34). Thus, liposome/immunoliposome delivery of epirubicin may provide potential clinical advantages.

In the U87/EGFRvIII model, free epirubicin at 24 mg/kg was associated with some antitumor efficacy, which was exceeded by that of the nontargeted liposomal version at equivalent drug dose (Fig. 4). The combination of liposomal epirubicin plus free mAb C225 showed enhanced efficacy as compared with liposomal epirubicin alone, consistent with preclinical and clinical results that C225 increases the efficacy of various chemotherapies (35). However, single-agent treatment with anti-EGFR immunoliposome-epirubicin at equivalent dose showed greater efficacy than all other treatments. Anti-EGFR immunoliposome-epirubicin was significantly superior to nontargeted liposomal epirubicin [P = 0.009, multivariate (rank) test], as well as to the combination of liposomal epirubicin plus free C225 ($P < 0.05$, individual two-sample t tests at three different time points).

Efficacy of anti–EGFR immunoliposomes containing alternative chemotherapy drugs. One of the theoretical advantages of immunoliposomal drug delivery versus other immunoconjugate approaches is the inherent versatility of the liposome component, which can be used to encapsulate various chemotherapeutic drugs or other compounds. To exploit this, we constructed anti-EGFR immunoliposomes containing either doxorubicin or vinorelbine; these were then directly compared for therapeutic effects *in vivo* in the EGFR-overexpressing U87 xenograft model (Fig. 5*A*).

For doxorubicin, anti-EGFR immunoliposome-doxorubicin was prepared from commercial PLD as described. Treatment with anti-EGFR immunoliposome-doxorubicin at a total drug dose of 15 mg/kg i.v. was associated with clear tumor regressions in this aggressive xenograft model and was significantly superior to treatment with nontargeted liposomal doxorubicin (P = 0.002; Fig. 5*B*).

For vinorelbine, a novel liposome construct was prepared by active loading across an induced transmembrane potential. Liposomal vinorelbine constructs achieved outstanding yields, with 26,000 drug molecules per nanoparticle, and stability, with prolonged drug retention during long circulation in rats ($t_{1/2}$ = 27.2 hours). Treatments with free, liposomal, or immunoliposomal vinorelbine were all administered i.v. at a total drug dose of 15 mg vinorelbine/kg (Fig. 5*C*). Liposomal vinorelbine seemed to have greater efficacy than free vinorelbine, although this comparison was of borderline statistical significance (P = 0.053). Anti-EGFR immunoliposome-vinorelbine showed a significant increase in efficacy over nontargeted liposomal vinorelbine (P = 0.003).

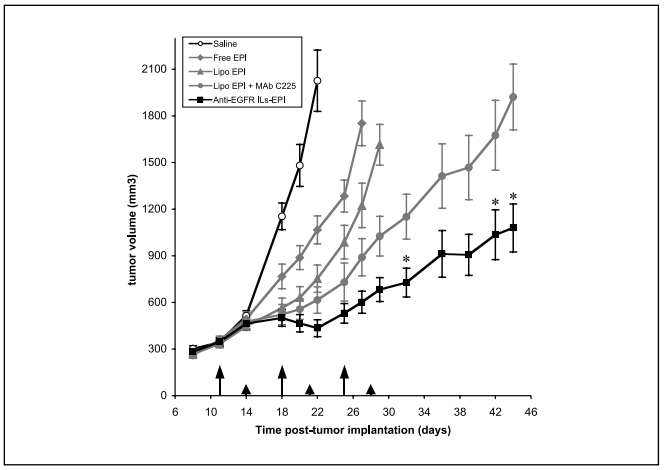

Figure 4. Therapeutic efficacy of anti-EGFR immunoliposomal epirubicin versus combination therapies in the U87/EGFRvIII tumor xenograft model. Anti-EGFR immunoliposomes containing epirubicin (*Anti-EGFR ILs-EPI*; ■) were administered i.v. once a week over 3 weeks at a total drug dose of 24 mg/kg on the indicated days post tumor implantation (*arrows*). Other treatment groups included saline (○), free epirubicin (*Free EPI*) at 24 mg/kg (◇), liposomal epirubicin at 24 mg/kg (*Lipo EPI*; ♦), and the combination of liposomal epirubicin at 24 mg/kg + free anti-EGFR mAb (*Lipo EPI + MAb C225*; ●) administered i.p. at 1 mg/dose twice a week over six doses (*small arrows*). Ten to twelve mice in each group. Anti-EGFR immunoliposome-epirubicin was significantly superior to liposomal epirubicin [P = 0.009, multivariate (rank) test] and was also superior to the combination of liposomal epirubicin + mAb C225 at the indicated time points (*, $P < 0.05$, individual two-sample t tests). *Points,* mean tumor volumes; *bars,* SE.

Comparison across the two drug classes showed that the efficacies of anti-EGFR immunoliposomes containing either doxorubicin or vinorelbine at 15 mg/kg of either drug were comparable (Fig. 5*A*). Similarly, the nontargeted liposomal versions of doxorubicin and vinorelbine, either commercial PLD or the new liposomal vinorelbine construct, were comparable to each other.

Discussion

Anti-EGFR immunoliposomes showed long circulation and stable drug retention, with no apparent compromise due to mAb fragment conjugation. Treatment studies with drug-loaded anti-EGFR immunoliposomes showed potent therapeutic effects in multiple tumor models, including tumor growth inhibition, regressions, and eradications. Anti-EGFR immunoliposomes loaded with doxorubicin, epirubicin, or vinorelbine were significantly superior to all other treatments, including the corresponding free drug, nontargeted liposomal drug, and other relevant comparators.

Of note, both nontargeted liposomes and anti-EGFR immunoliposomes showed largely comparable biodistributions at the tissue level. Both types of nanoparticles achieved extremely high tumor concentrations at 24 hours (10-12% ID/g tissue) and even higher levels at 72 hours (13-15% ID/g tissue). Hence, whereas drug-loaded immunoliposomes produced clearly greater antitumor efficacy than nontargeted versions, targeting was not associated with increased tumor tissue levels.

This apparent paradox, also observed with anti-HER2 immunoliposomes in HER2-overexpressing tumors (23), was clarified by further studies of the mechanism of delivery for liposomes and immunoliposomes at the cellular level. We previously

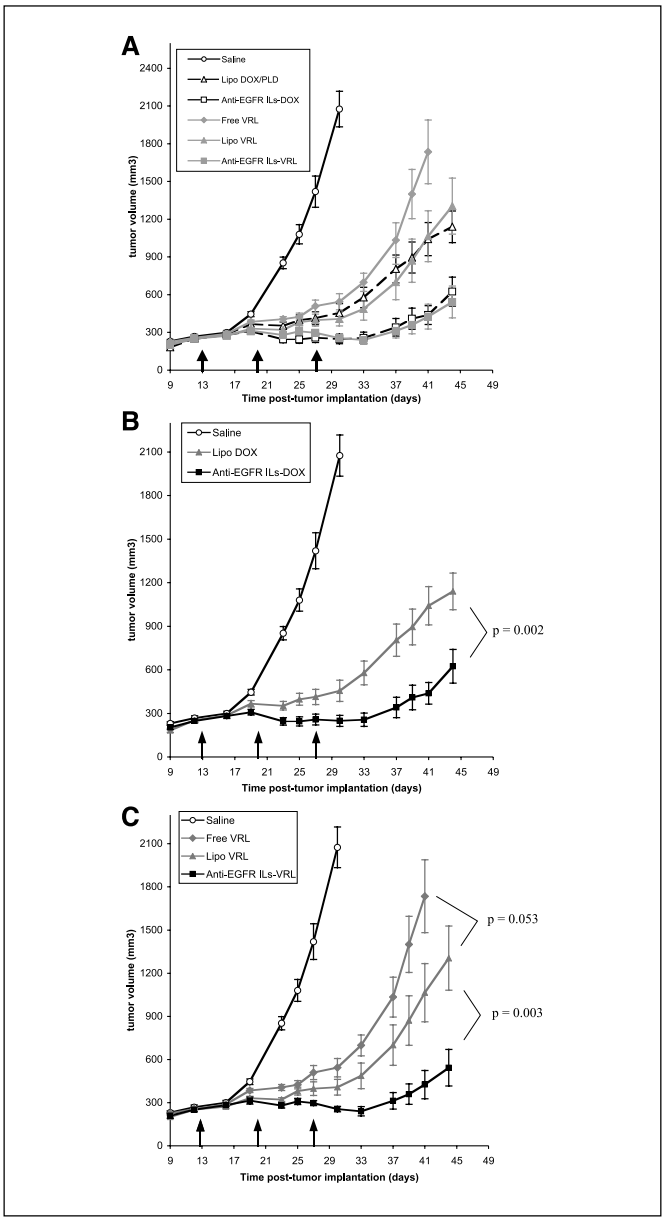

Figure 5. Efficacy of anti-EGFR immunoliposomes containing various drugs in the U87 tumor xenograft model. *A,* all treatments. Two cytotoxic drugs with different mechanisms of action were encapsulated into liposomes or anti-EGFR immunoliposomes: doxorubicin and vinorelbine (*VRL*). For each of these drug classes, nude mice with flank U87 tumor xenografts were treated with saline, free drug, nontargeted liposomal drug, or anti-EGFR immunoliposomal drug. Each group contained 10 to 12 tumor-bearing mice. *Points,* mean tumor volumes; *bars,* SE. Pairwise comparisons of treatments were done by multivariate (rank) test. For clarity, treatment results for each set of drugs are shown separately in (*B* and *C*). *B,* doxorubicin. Anti-EGFR immunoliposome-doxorubicin (*Anti-EGFR ILs-DOX*; ■) was prepared by micellar conjugation of Fab′ to commercial PLD (*Lipo DOX/PLD*; ♦), and both were administered i.v. at a total doxorubicin dose of 15 mg/kg over three doses (*arrows*). Anti-EGFR immunoliposome-doxorubicin was significantly superior to nontargeted PLD ($P = 0.002$). *C,* vinorelbine. Nanoparticle/liposome constructs encapsulating vinorelbine were prepared via induced transmembrane potential for active drug loading, resulting in highly concentrated drug packing of 26,000 drugs per particle. Anti-EGFR immunoliposomes containing vinorelbine (*Anti-EGFR ILs-VRL*; ■) were administered i.v. at a total dose of 15 mg/kg on the indicated days post tumor implantation (*arrows*). Other treatment groups included saline (○), free vinorelbine (◇), and liposomal vinorelbine (*Lipo VRL*; ♦), both at 15 mg vinorelbine/kg. There was a trend towards superior efficacy for liposomal vinorelbine over free vinorelbine ($P = 0.053$) whereas anti-EGFR immunoliposome-vinorelbine was in turn clearly superior to nontargeted liposomal vinorelbine ($P = 0.003$).

reported that anti-EGFR immunoliposomes bind and internalize in EGFR-overexpressing tumor cells *in vitro*, thus enabling intracellular drug delivery (10). The present studies confirm that immunoliposomes internalize in target cells *in vivo*. Tumor cells analyzed after i.v. treatment showed internalization of immunoliposomes but not of nontargeted liposomes. These data are consistent with a mechanism for immunoliposome delivery involving two phases. In the first or tissue phase, nanoparticles with sufficient longevity in circulation (such as sterically stabilized liposomes or immunoliposomes) slowly accumulate in tumor tissue, ultimately reaching high tumor levels due to the enhanced permeability and retention effect. Molecular targeting is not required for this process and does not seem to facilitate it. In the second or cellular phase, nontargeted liposomes remain in the interstitial space and are subject to decomposition, degradation, or phagocytosis, with eventual release of drug. In contrast, immunoliposomes bind to and internalize in tumor cells via ligand-receptor interactions. Taken together, these results indicate that internalization of anti-EGFR immunoliposomes in tumor cells was a critical factor for the enhanced efficacy observed.

It was also clear that anti-EGFR immunoliposome efficacy was not attributable to signal inhibition mediated by the C225 component. Empty anti-EGFR immunoliposomes, administered at the same lipid dose and schedule as doxorubicin-loaded immunoliposomes, failed to show antitumor efficacy. This was in fact not surprising given the large difference in the dose requirements involved. Treatment with free mAb C225 required 1,000 μg per dose for six doses. Immunoliposome treatment, in contrast, required very small amounts of conjugated mAb fragments: ~30 μg Fab′ per dose for three doses, corresponding to more than 60-fold lower mAb content. It is also notable that anti-EGFR immunoliposomes showed greater efficacy than the combination of free C225 plus liposomal epirubicin.

Immunoliposomal drugs may provide a more potent strategy to treat EGFR-overexpressing tumors than current approaches. Strategies to inhibit EGFR signal transduction, including naked mAbs and small molecule inhibitors, have proved to be clinically useful (36–39); however, it remains unclear which subsets of patients are most likely to receive clinical benefit from these treatments (40, 41). Anti-EGFR immunoliposomes can target both wild-type EGFR and EGFRvIII and their efficacy is not dependent on signal transduction effects.

In conclusion, anti-EGFR immunoliposomes achieved favorable pharmacokinetics, biodistribution, and tumor localization due to its nanoparticle properties, followed by specific binding and internalization in tumor cells via mAb fragments. Targeting different drugs to tumor cells in this way produced potent anticancer activity in preclinical models, thus representing a potentially useful strategy for cancer treatment.

Acknowledgments

Received 3/31/2005; revised 10/3/2005; accepted 10/7/2005.

Grant support: National Cancer Institute Specialized Programs of Research Excellence in Breast Cancer (grant P50-CA58207) and Brain Tumors (grant P50-CA097257), Accelerated Brain Cancer Cure (ABC2), and Expedition Inspiration; The Swiss Academy of Medical Sciences/Swiss National Science Foundation, Novartis Foundation, Swiss Cancer League, and Cancer League of Basel, Switzerland (C. Mamot); and New Investigator Award from California's Breast Cancer Research Program of the University of California, grant 7KB-0066 (D.C. Drummond).

The costs of publication of this article were defrayed in part by the payment of page charges. This article must therefore be hereby marked *advertisement* in accordance with 18 U.S.C. Section 1734 solely to indicate this fact.

References

1. Allen TM, Cullis PR. Drug delivery systems: entering the mainstream. Science 2004;19:1818–22.
2. Noble CO, Kirpotin DB, Hayes ME, et al. Development of ligand-targeted liposomes for cancer therapy. Expert Opin Ther Targets 2004;8:335–53.
3. Park JW, Hong K, Kirpotin DB, Papahadjopoulos D, Benz CC. Immunoliposomes for cancer treatment. Adv Pharmacol 1997;40:399–435.
4. Park JW, Hong K, Carter P, et al. Development of anti-p185HER2 immunoliposomes for cancer therapy. Proc Natl Acad Sci U S A 1995;92:1327–31.
5. Kirpotin D, Park JW, Hong K, et al. Sterically stabilized anti-HER2 immunoliposomes: design and targeting to human breast cancer cells *in vitro*. Biochemistry 1997; 36:66–75.
6. Park JW, Hong K, Kirpotin DB, et al. Anti-HER2 Immunoliposomes: Enhanced Efficacy Attributable to Targeted Delivery. Clin Cancer Res 2002;8:1172–81.
7. Nellis DF, Ekstrom DL, Kirpotin DB, et al. Preclinical manufacture of an anti-HER2 scFv-PEG-DSPE, liposome-inserting conjugate. 1. Gram-scale production and purification. Biotechnol Prog 2005;21:205–20.
8. Nellis DF, Kirpotin DB, Janini GM, et al. Preclinical manufacture of anti-HER2 liposome-inserting, scFv-PEG-lipid conjugate. 2. Conjugate micelle identity, purity, stability, and potency analysis. Biotechnol Prog 2005;21:221–32.
9. Mendelsohn J, Baselga J. Status of epidermal growth factor receptor antagonists in the biology and treatment of cancer. J Clin Oncol 2003;21:2787–99.
10. Mamot C, Drummond DC, Greiser U, et al. Epidermal growth factor receptor (EGFR)-targeted immunoliposomes mediate specific and efficient drug delivery to EGFR- and EGFRvIII-overexpressing tumor cells. Cancer Res 2003;63:3154–61.
11. Szoka F, Jr., Papahadjopoulos D. Comparative properties and methods of preparation of lipid vesicles (liposomes). Annu Rev Biophys Bioeng 1980;9:467–508.
12. Bartlett GR. Phosphorus Assay in Column Chromatography. J Biol Chem 1959;234:466–8.
13. Lasic DD, Frederik PM, Stuart MC, Barenholz Y, McIntosh TJ. Gelation of liposome interior. A novel method for drug encapsulation. FEBS Lett 1992;312:255–8.
14. Haran G, Cohen R, Bar LK, Barenholz Y. Transmembrane ammonium sulfate gradients in liposomes produce efficient and stable entrapment of amphipathic weak bases. Biochim Biophys Acta 1993;1151:201–15.
15. Sonoda Y, Ozawa T, Hirose Y, et al. Formation of intracranial tumors by genetically modified human astrocytes defines four pathways critical in the development of human anaplastic astrocytoma. Cancer Res 2001;61:4956–60.
16. Prewett MC, Hooper AT, Bassi R, Ellis LM, Waksal HW, Hicklin DJ. Enhanced antitumor activity of anti-epidermal growth factor receptor monoclonal antibody IMC-C225 in combination with irinotecan (CPT-11) against human colorectal tumor xenografts. Clin Cancer Res 2002;8:994–1003.
17. O'Brien PC. Procedures for comparing samples with multiple end points. Biometrics 1984;40:1079–87.
18. Iden DL, Allen TM. *In vitro* and *in vivo* comparison of immunoliposomes made by conventional coupling techniques with those made by a new post-insertion approach. Biochim Biophys Acta 2001;1513:207–16.
19. Drummond DC, Meyer O, Hong K, Kirpotin DB, Papahadjopoulos D. Optimizing liposomes for delivery of chemotherapeutic agents to solid tumors. Pharmacol Rev 1999;51:691–743.
20. Drummond D, Noble CO, Guo Z, et al. Development of a highly stable liposomal irinotecan with low toxicity and potent antitumor efficacy. Proc Am Assoc Cancer Res 2005; abstr 1409.
21. Drummond D, Noble CO, Mamot C, et al. Development of novel liposomal and receptor tyrosine kinase-targeted immunoliposomal vinorelbine formulations with improved drug retention. Proc Am Assoc Cancer Res 2005; abstr 4394.
22. Gabizon A, Shiota R, Papahadjopoulos D. Pharmacokinetics and tissue distribution of doxorubicin encapsulated in stable liposomes with long circulation times. J Natl Cancer Inst 1989;81:1484–8.
23. Park JW, Kirpotin DB, Hong K, et al. Anti-HER2 immunoliposomes: enhanced efficacy via intracellular delivery [abstract]. Proc Am Assoc Cancer Res 2000;41:524.
24. Huang HS, Nagane M, Klingbeil CK, et al. The enhanced tumorigenic activity of a mutant epidermal growth factor receptor common in human cancers is mediated by threshold levels of constitutive tyrosine phosphorylation and unattenuated signaling. J Biol Chem 1997;272:2927–35.
25. Wikstrand CJ, McLendon RE, Friedman AH, Bigner DD. Cell surface localization and density of the tumor-associated variant of the epidermal growth factor receptor, EGFRvIII. Cancer Res 1997;57:4130–40.
26. Tang CK, Gong XQ, Moscatello DK, Wong AJ, Lippman ME. Epidermal growth factor receptor vIII enhances tumorigenicity in human breast cancer. Cancer Res 2000;60:3081–7.
27. Humphrey PA, Wong AJ, Vogelstein B, et al. Amplification and expression of the epidermal growth factor receptor gene in human glioma xenografts. Cancer Res 1988;48:2231–8.
28. Wikstrand CJ, Hale LP, Batra SK, et al. Monoclonal antibodies against EGFRvIII are tumor specific and react with breast and lung carcinomas and malignant gliomas. Cancer Res 1995;55:3140–8.
29. Yamazaki H, Fukui Y, Ueyama Y, et al. Amplification of the structurally and functionally altered epidermal growth factor receptor gene (c-erbB) in human brain tumors. Mol Cell Biol 1988;8:1816–20.
30. Okamoto I, Kenyon LC, Emlet DR, et al. Expression of constitutively activated EGFRvIII in non-small cell lung cancer. Cancer Sci 2003;94:50–6.
31. Rae JM, Scheys JO, Clark KM, Chadwick RB, Kiefer MC, Lippman ME. EGFR and EGFRvIII expression in primary breast cancer and cell lines. Breast Cancer Res Treat 2004;87:87–95.
32. Minotti G, Menna P, Salvatorelli E, Cairo G, Gianni L. Anthracyclines: molecular advances and pharmacologic developments in antitumor activity and cardiotoxicity. Pharmacol Rev 2004;56:185–229.
33. Mross K, Niemann B, Massing U, et al. Pharmacokinetics of liposomal doxorubicin (TLC-D99; Myocet) in patients with solid tumors: an open-label, single-dose study. Cancer Chemother Pharmacol 2004;54:514–24.
34. O'Brien ME, Wigler N, Inbar M, et al. Reduced cardiotoxicity and comparable efficacy in a phase III trial of pegylated liposomal doxorubicin HCl (CAELYX/Doxil) versus conventional doxorubicin for first-line treatment of metastatic breast cancer. Ann Oncol 2004; 15:440–9.
35. Baselga J. The EGFR as a target for anticancer therapy-focus on cetuximab. Eur J Cancer 2001;37 Suppl 4:S16–22.
36. Goldstein NI, Prewett M, Zuklys K, Rockwell P, Mendelsohn J. Biological efficacy of a chimeric antibody to the epidermal growth factor receptor in a human tumor xenograft model. Clin Cancer Res 1995;1: 1311–8.
37. Overholser JP, Prewett MC, Hooper AT, Waksal HW, Hicklin DJ. Epidermal growth factor receptor blockade by antibody IMC-C225 inhibits growth of a human pancreatic carcinoma xenograft in nude mice. Cancer 2000;89:74–82.
38. Kris MG, Natale RB, Herbst RS, et al. Efficacy of gefitinib, an inhibitor of the epidermal growth factor receptor tyrosine kinase, in symptomatic patients with non-small cell lung cancer: a randomized trial. JAMA 2003;290:2149–58.
39. Fukuoka M, Yano S, Giaccone G, et al. Multi-institutional randomized phase II trial of gefitinib for previously treated patients with advanced non-small-cell lung cancer. J Clin Oncol 2003;21:2237–46.
40. Lynch TJ, Bell DW, Sordella R, et al. Activating mutations in the epidermal growth factor receptor underlying responsiveness of non-small-cell lung cancer to gefitinib. N Engl J Med 2004;350:2129–39.
41. Paez JG, Janne PA, Lee JC, et al. EGFR mutations in lung cancer: correlation with clinical response to gefitinib therapy. Science 2004;304:1497–500.

Epidermal Growth Factor Receptor–Targeted Immunoliposomes Significantly Enhance the Efficacy of Multiple Anticancer Drugs *In vivo*

Christoph Mamot, Daryl C. Drummond, Charles O. Noble, et al.

Cancer Res 2005;65:11631-11638.